Simple Autonomous Chaotic Circuits

Jessica R. Piper, *Student Member, IEEE*, and J. C. Sprott

***Abstract*—Over the last several decades, numerous electronic circuits exhibiting chaos have been proposed. Nonautonomous circuits with as few as two physical components have been developed. However, the operation of such circuits has typically traded physical simplicity for analytic complexity, or vice versa. In this brief, we present two simple autonomous chaotic circuits using only op-amps and linear time-invariant passive components. Each circuit employs one op-amp as a comparator to provide signum nonlinearity. The chaotic behavior is robust, and the circuits offer simple analysis, while minimizing both physical and model component counts.**

***Index Terms*—Chaos, nonlinear circuits, oscillators.**

I. Introduction

OVER THE last three decades, many chaotic circuits have been proposed, and there has been an ongoing debate over which one is the "simplest" example of chaos. As is typical in such debates, there has not been a decisive winner. The debate has been complicated by the lack of a widely accepted definition of exactly what constitutes a simple circuit. Furthermore, there have actually been two parallel debates: for the simplest nonautonomous (driven) and the simplest autonomous circuits.

For the purposes of this brief, we will consider three kinds of simplicity. The first is mathematical simplicity, where we can gauge how simple a class of function is roughly by when it is covered in mathematics education. For example, algebraic functions are simpler than exponentials. Likewise, time-invariant systems are preferred over time-varying systems. Second, a simple circuit should minimize both the number of physical components and the number of idealized elements required to accurately model the circuit. Third, we consider simplicity from a practical standpoint, preferring robust standalone circuits that can be constructed using the most common components.

Based on our third qualification of simplicity, autonomous circuits are preferred. However, we will begin our review of the literature with nonautonomous circuits because this is where the debate got its start.

Linsay's driven inductor–varactor resonator is one of the first simple chaotic circuits [1]. By employing the output resistance of the driving generator, Linsay's circuit uses only two physical components. One might think that Linsay had won the race before anyone else had left the gate. However, the chaos in Linsay's circuit relies on the nonlinear capacitance of the diode. Therefore, the mathematical model of the circuit is fairly complex.

Deane's nonlinear resistance–inductance–capacitance circuit [2] is a particularly interesting but often overlooked case of chaos in a passive circuit. It relies on the saturation of an iron core inductor for its nonlinearity. Therefore, the model inductance changes in time and exhibits hysteresis (memory) effects.

The system proposed by Murali *et al.* [3] uses only three components on paper, but the nonlinear resistor alone requires ten active and passive devices to model. However, in contrast to the previously mentioned contenders, the mathematical analysis of the Murali–Lakshmanan–Chua circuit relies on piecewise-linear algebraic functions, so it is mathematically simpler.

One of the most recent claims to simplest nonautonomous chaos is Lindberg *et al.*'s single-transistor chaotic resonator [4]. This circuit uses one transistor, two resistors, and one or two capacitors. The operation is based on a mechanism that Lindberg *et al.* characterize as "integration interruption," which uses both forward and reverse active transistor modes.

In the realm of autonomous circuits, Chua's circuit was among the first to be proposed [5]. Chua's circuit has the benefits of mathematical simplicity (via piecewise linear algebraic functions), but as with its nonautonomous variant mentioned previously, the physical component count is not minimized.

Tsubone and Saito [6] proposed a second-order system that is driven to chaos by the action of a hysteretic switch. While the system equation is simple, the hysteresis in the switching condition means that the system is not time invariant. In addition, their circuit is relatively elaborate.

In the last decade, chaotic systems written as jerk equations have come into fashion. Jerk equations offer an exceptionally simple notation for higher order systems. One system that has received considerable attention [7], [8] is

$$\dddot{x} + A\ddot{x} + B\dot{x} = C\left(\mathrm{sgn}(x) - x\right) \tag{1}$$

where the signum function $\mathrm{sgn}(x)$, which can be conveniently approximated using an op-amp without negative feedback, is defined as

$$\mathrm{sgn}(x) = \begin{cases} -1, & \text{for } x < 0 \\ 0, & \text{for } x = 0 \\ 1, & \text{for } x > 0. \end{cases} \tag{2}$$

Elwakil and Kennedy [8] implemented the system of (1) using a state variable topology. This topology requires one op-amp for each integration or gain block, so that it

Manuscript received February 12, 2010; revised April 19, 2010; accepted June 7, 2010. Date of publication August 30, 2010; date of current version September 15, 2010. The work of J. Piper was supported by the National Science Foundation under Grant CCF-0649235. This paper was recommended by Associate Editor A. Brambilla.

J. Piper was with the Department of Electrical and Computer Engineering, University of Massachusetts, Lowell, MA 01854 USA. She is now with the Department of Electrical Engineering, Stanford University, Stanford, CA 94305 USA (e-mail: jrylan@stanford.edu).

J. C. Sprott is with the Department of Physics, University of Wisconsin, Madison, WI 53706 USA (e-mail: sprott@physics.wisc.edu).

Digital Object Identifier 10.1109/TCSII.2010.2058493

trades simplicity of analysis for increased component count. Specifically, the circuit in [8] requires eight resistors, three capacitors, and five op-amps. By making one of the integration stages purely passive, Sprott [7] reduced the component count for a variant of this system to five resistors, three capacitors, and three op-amps.

In this brief, we examine two further simplified realizations of (1), each using one active integrator and a passive second-order integrator. The first, which for shorthand we refer to as *CCC*, uses four resistors, three capacitors, and two op-amps. The second, which we designate *CLC*, uses two resistors, two capacitors, one inductor, and two op-amps. These circuits were proposed in [10], although not tested.

II. Analysis of the System

Using the phase variable $\mathbf{x} = [x_1, x_2, x_3]^T$, we can rewrite the system equation (1) as

$$\dot{\mathbf{x}} = \begin{bmatrix} 0 & 1 & 0 \\ 0 & 0 & 1 \\ -C & -B & -A \end{bmatrix} \mathbf{x} + \begin{bmatrix} 0 \\ 0 \\ C\mathrm{sgn}(x_1) \end{bmatrix}. \tag{3}$$

For the purpose of analysis, (3) can be divided into three linear regions, which are piecewise continuous. Specifically, we consider an inner region arbitrarily close to the origin (where $|x_1| < \epsilon$ for some arbitrarily small positive constant ϵ) and two outer regions where x_1 is well away from the origin. In the outer regions, the term $C\mathrm{sgn}(x_1)$ is simply a constant. Thus, the outer regions are defined by two affine equations with the same Jacobian as (3), and they have the same eigenvalues.

In the inner region, we connect the two outer regions with a straight line, so that

$$\mathrm{sgn}(x_1) - x_1 \approx x_1/\epsilon, \quad \text{for } |x_1| < \epsilon.$$

Therefore, in this inner region, the constant term disappears, and the system equation is

$$\dot{\mathbf{x}} = \begin{bmatrix} 0 & 1 & 0 \\ 0 & 0 & 1 \\ C/\epsilon & -B & -A \end{bmatrix} \mathbf{x}. \tag{4}$$

In the circuit implementations, A, B, and C are functions of the passive components, which all have positive real values. Furthermore, both the CCC and CLC circuits have a similar distribution of eigenvalues. In the outer regions, there are a single negative real eigenvalue γ and a complex conjugate pair of eigenvalues with positive real part σ. In the central region, the real eigenvalue γ is positive, while the real part of the complex conjugate pair σ is negative.

In a qualitative sense, the negative real eigenvalues in the outer regions provide direct-current sinks to the critical points at $\mathbf{x} = (\pm 1, 0, 0)$, but the positive σ causes increasing oscillation about these points. When the amplitude of oscillation grows big enough to bring $\mathbf{x}$ into the neighborhood of the critical point at (0, 0, 0), the large positive real eigenvalue acts as a repeller, "shooting" the trajectory out of the inner region.

For the purpose of simulation, we instead model the signum function as $k\tanh(Mx)$, where larger values of M more closely approximate $\mathrm{sgn}(x)$, and the constant k represents the total voltage swing of the comparator, which, for real op-amps, will be less than the total supply voltage. This approximation is helpful because $\tanh(Mx)$ is continuous and differentiable, and, furthermore, its derivative is continuous.

The two circuits were simulated using the semi-implicit Crank–Nicholson algorithm, using an absolute error tolerance of 10^{-12}, relative error tolerance of 10^{-4}, and an initial time increment of 50 μs. The simulations were run for 100 000 points, corresponding to 5 s of simulation time, and the first 2.5 s was thrown away to dispense with transients related to the initial conditions.

III. CCC Case

In the circuit in Fig. 1(a), R_1-C_2-R_2-C_3 forms the passive second-order integrator, while R_c-R-C_1-$U1a$ forms the active integrator. Applying nodal analysis, and considering VC_3 as the phase variable x_1, this circuit solves (1) with the parameters given by

$$A = \frac{R + R_2}{RR_2C_3} + \frac{R_1 + R_2}{R_1R_2C_2} \tag{5}$$

$$B = \frac{R + R_1 + R_2}{RR_1R_2C_2C_3} \tag{6}$$

$$C = \frac{1}{RR_1R_2C_1C_2C_3}. \tag{7}$$

A practical version of the circuit can be built with $R_1 = R_2 = 47$ kΩ, $R = 100$ kΩ variable, $R_C = 1$ MΩ, $C_1 = 1$ nF, $C_2 = 10$ nF, and $C_3 = 20$ nF. For $R = 27.8$ kΩ, $A = 6.86\text{E}3$ s^{-1}, $B = 9.02\text{E}6$ s^{-2}, and $C = 7.40\text{E}10$ s^{-3}. Depending on the setting of the bifurcation parameter R, the primary observed frequency will be in the range of 350–550 Hz. At some settings of R, there will also be strong low-frequency components (in the range of 2 Hz) as the trajectory slowly jumps between lobes.

The circuit was constructed using a TL084 quad op-amp, powered by a single 9v battery. The two extra sections of the op-amp were used to buffer the voltages of capacitors C_2 and C_3. A TLE2426 "rail splitter" was used to generate a ground reference for the circuit, but similar results are obtained using a resistive voltage divider of two 10k resistors and suitable bypass capacitors. Alternately, one could use two batteries to make a bipolar supply.

The comparator resistor R_C needs to be scaled according to the output swing of the comparator op-amp in order to prevent saturation of the integrator. For the TL084 run from a single 9v supply, the observed saturation voltages were $+3.76$v and -2.96v. This asymmetry was included in the numerical model as an output swing of ± 3.36 V and an offset of 0.4 V, but no attempt was made to model the slew rate or the input impedance of the op-amp.

As R is increased, the real eigenvalue migrates toward the origin. For the complex conjugate eigenvalues, ω decreases in magnitude as R is increased, while σ crosses into the right half-plane around $R = 15$ kΩ, increases to a maximum of 106 around $R = 20$ kΩ, and then decreases and returns to the left half-plane around $R = 70$ kΩ. Referring to the bifurcation

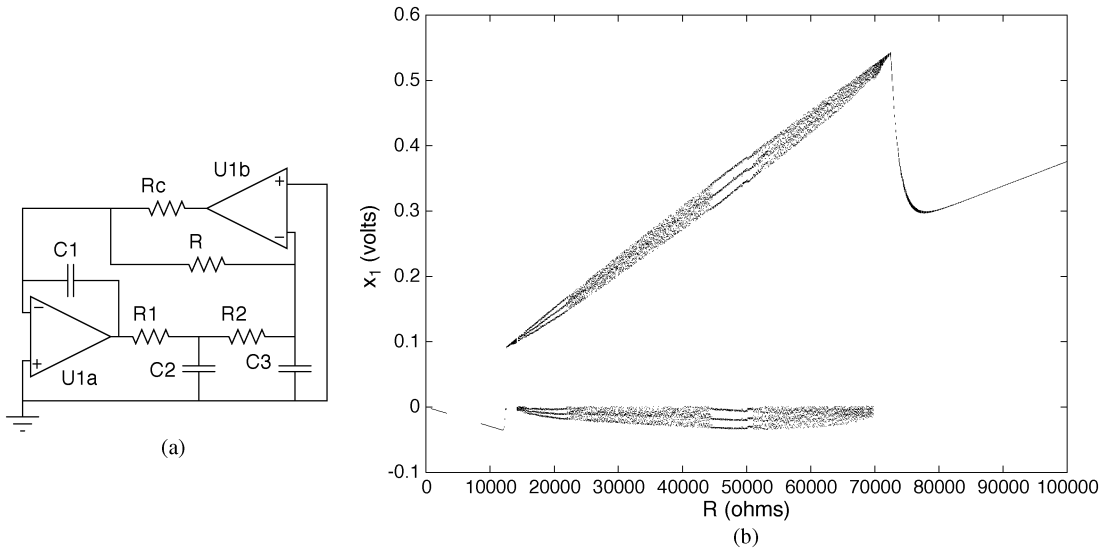

Fig. 1. CCC circuit. (a) CCC schematic. (b) Theoretical bifurcation diagram for the CCC circuit.

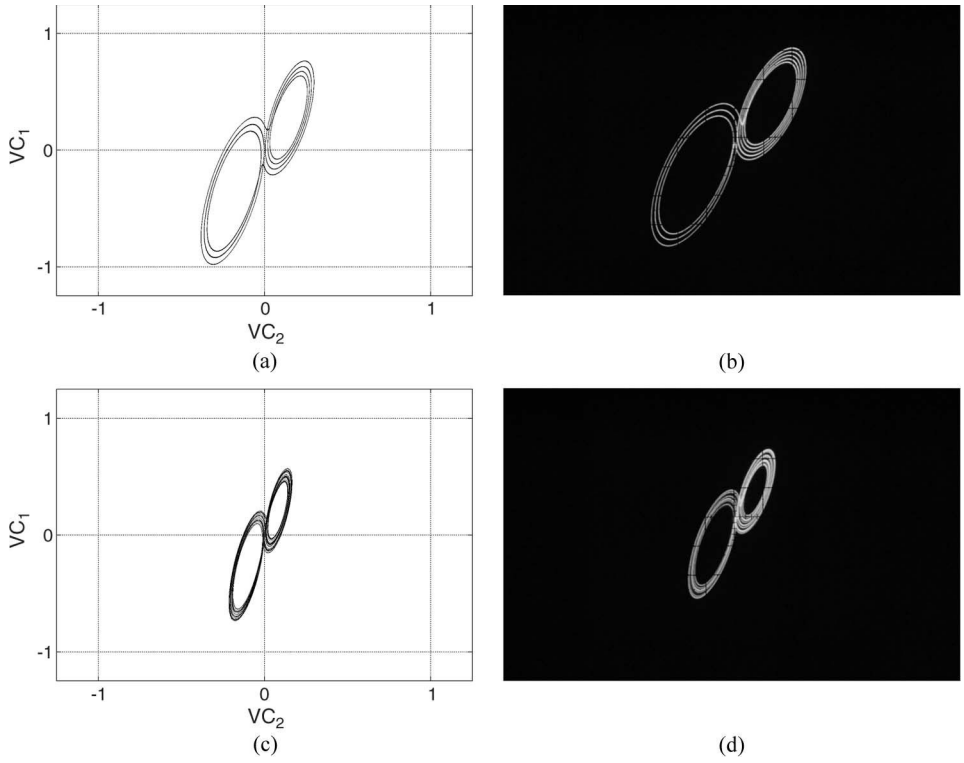

Fig. 2. VC_2 versus VC_3 for several values of R, CCC circuit: (a), (c) are from simulation; (b), (d) are oscilloscope photos of the circuit output. (a) $R = 49.8$ kΩ. (b) $R = 49.8$ kΩ. (c) $R = 27.8$ kΩ. (d) $R = 27.8$ kΩ.

diagram Fig. 1(b), the onset and the demise of chaos correspond to $\sigma > 0$.

Fig. 2 shows comparison plots in the VC_3-VC_2 plane between the simulated and observed behavior for several values of R. For $R = 49.8$ kΩ, the solutions of both the simulation and the physical circuit are stable, although as seen in the plots, the physical circuit has one extra loop in the upper lobe. Numerical experiments indicated that while the location of the stable region was controlled by the bifurcation parameter R, the detail of the structure was dependent on the effective offset of the comparator. For $R = 27.8$ kΩ, both the simulation and the circuit exhibit chaos. For the chaotic attractor shown in Fig. 2(c), the Lyapunov exponent spectrum was calculated as $\lambda = \langle 0.1880, 0, -7.045 \rangle\ (\text{ms})^{-1}$, following the procedure in [9].

At the upper end of the range of R, a sinusoidal solution was observed in both the simulation and the experiment; however, the value of R in the simulation was greater than R for stable oscillation in the circuit (not shown). Likewise, stable R was less in the simulation than in experiment at the other end of the range. This spreading is likely due to dissipation in the physical circuit, which does not exist in the model. Referring again to the bifurcation diagram [see Fig. 1(b)], periodic solutions are

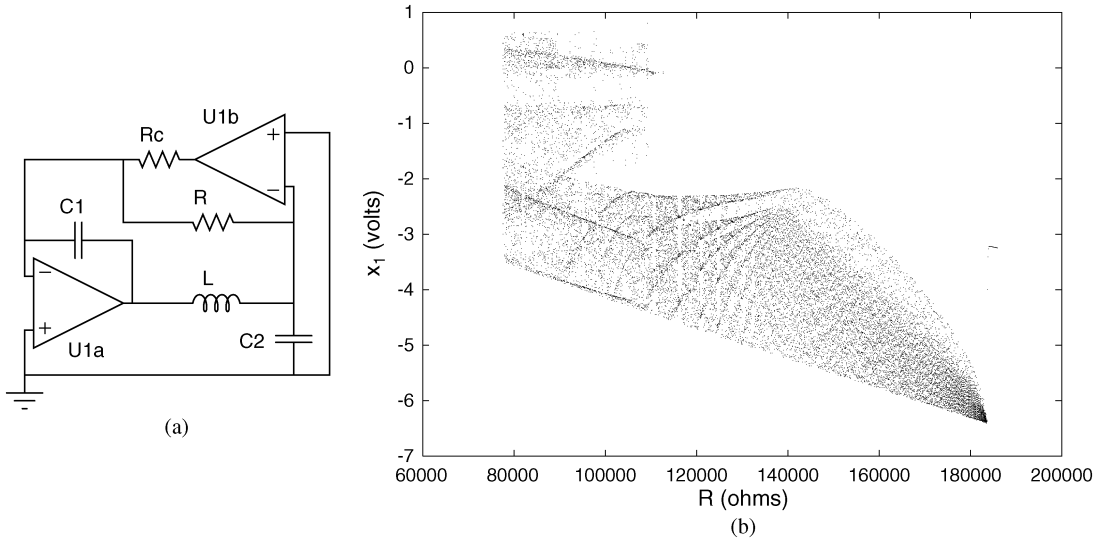

Fig. 3. CLC circuit. (a) CLC schematic. (b) Theoretical bifurcation diagram for the CLC circuit.

predicted by the model around $R = 20$ kΩ, but no stable region was observed in the physical circuit around that value of R.

IV. CLC Case

The circuit for the CLC case is given in Fig. 3(a). Here, L-C_2 forms the second-order passive integrator. To avoid the nonlinear and hysteresis effects of core saturation, an air-core inductor was employed. The inductor used in the test circuit was quite compact, measuring 1.5 cm tall by 1.1 cm in diameter. The series resistance of the inductor R_L was included in the model. The circuit parameters are given by

$$A = R_L/L + 1/RC_2 \tag{8}$$

$$B = (1 + R_L/R)/LC_2 \tag{9}$$

$$C = 1/RC_1LC_2. \tag{10}$$

The circuit was constructed with $C_1 = 4.7$ nF, $C_2 = 1$ μF, $L = 0.1$ H, $R_L = 105$ Ω, $R_C = 475$ kΩ, and R variable from 68k to 168k (a precision 100k potentiometer was used in series with a fixed 68k resistor). Note that for the inductor used, R_L/L dominates A, whereas R_L/R can be neglected in B, so that the parameters A and B can be treated as constants. However, R_L has a strong effect on the eigenvalues, and as R_L decreases, the real part σ of the complex conjugate pair increases. For inductors with different series resistance, the component values will need to be adjusted to achieve bounded chaos. For the given components, $A = 1.15\text{E}3$ s^{-1}, $B = 1.08\text{E}7$ s^{-2}, and C ranges between about 2.9E10 and 1.4E10 s^{-3}. In many regions, there is a strong frequency component around 510 Hz, although in the chaotic regions, the spectrum is considerably more spread out than in the CCC case.

A TL084 op-amp was used, running from a bipolar $\pm$9v supply. The output of the comparator op-amp was $+8.2$v and -7.8v. The amplitude and the offset were included in the CLC simulation, but the effects of the op-amp input impedance and the slew rate were neglected. All simulated runs were started with initial conditions $x_1 < 0$, $x_2 = x_3 = 0$. The outputs taken from the circuit were VC_2, corresponding to x_1, and VC_1, corresponding to $(1 + R_L/R)x_1 + (R_LC_2 + L/R)x_2 + LC_2x_3$.

As R is decreased, both the inner and outer region eigenvalues migrate away from the origin. The real part of the outer complex conjugate eigenvalues crosses the imaginary axis around $R = 186$ kΩ, corresponding to the bounded solution at the right of the bifurcation diagram [see Fig. 3(b)]. For $R < 75$ kΩ, the solution becomes unbounded. The maximum value of σ for a bounded solution is around 500, considerably larger than in the CCC circuit.

Several typical chaotic and periodic phase portraits in the VC_2-VC_1 plane are shown in Fig. 4. The simulated and experimental results agreed closely. In contrast to the CCC circuit, the experimental CLC circuit exhibited many stable regions, including (in addition to those shown) periods 2 and 7 on a single lobe, doubled orbits of 6, 8, 10, and 12 on a single lobe, as well as more complicated periods occupying both lobes. For the chaotic region with $R = 79.0$ kΩ shown in Fig. 4(a), the Lyapunov exponent spectrum was calculated as $\lambda = \langle 0.3937, 0, -1.5536\rangle$ (ms)$^{-1}$.

It is worth remarking that while the solutions for $R > 140$ kΩ presented in Fig. 4 all reside on the bottom lobe, symmetric solutions lying on the upper lobe are also possible, given initial conditions where $x_1 > 0$, $x_2 = x_3 = 0$. Indeed, on startup, with R initially set to 168 kΩ and gradually lowered, the experimental circuit solutions remain on the upper lobe until around $R = 138$ kΩ, where they flip to the bottom lobe. The solutions for $R < 140$ kΩ are not effected by initial conditions.

V. Conclusion

As outlined in Section I, different definitions of what constitutes a simple chaotic circuit have been proposed during this 30-year debate. All of the previous examples have pushed the current state of the art and increased our fundamental understanding of the phenomena of chaos. Therefore, picking a "winner" is something of a moot point.

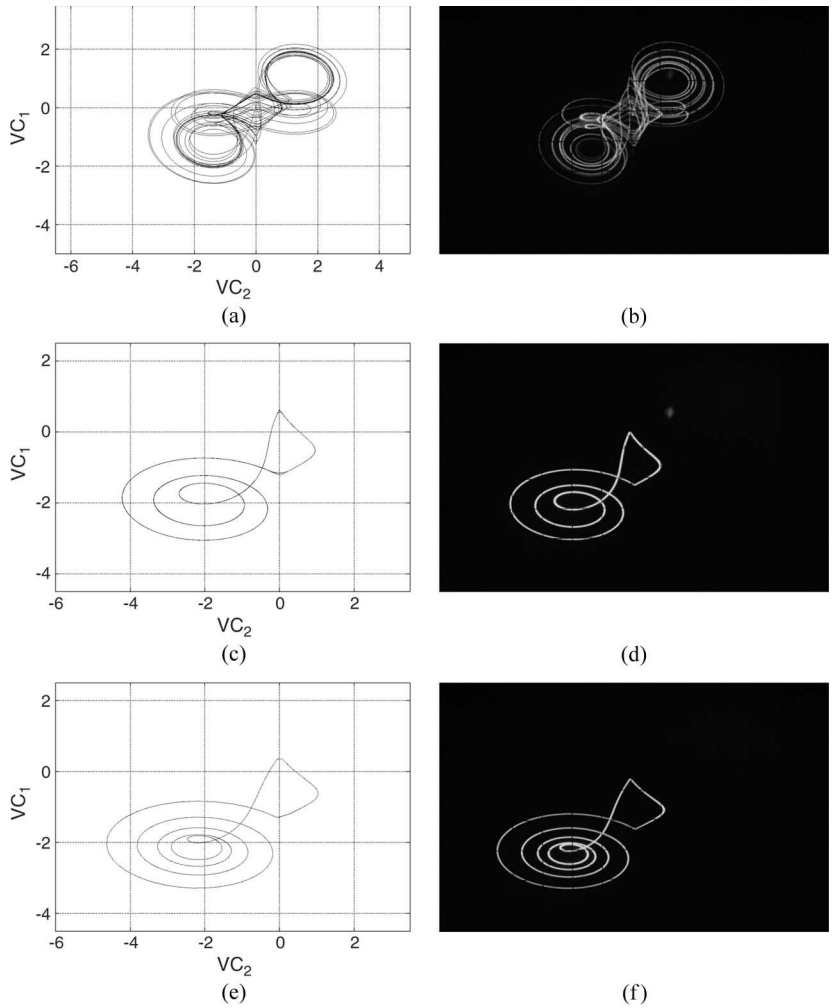

Fig. 4. Simulation and experiment for CLC, VC_2-VC_1 plane. (a), (b) Chaotic solution on two lobes. (c), (d) Period 3 on a single lobe. (e), (f) Period 5 on a single lobe. (a) $R = 79.0\,\text{k}\Omega$. (b) $R = 79.0\,\text{k}\Omega$. (c) $R = 116.5\,\text{k}\Omega$. (d) $R = 113.9\,\text{k}\Omega$. (e) $R = 124.9\,\text{k}\Omega$. (f) $R = 122.9\,\text{k}\Omega$.

On the other hand, the circuits described in this brief offer several practical advantages. First, the system equation is straightforward, and the nonlinearity is simply defined. Second, the passive components are strictly linear and time invariant. Third, both physical and model component counts are minimized.

However, most importantly, the present circuits are general and robust. That is, one can buy all the parts to successfully construct either circuit at Radio Shack, with minimal substitution. Tolerances and layout are not particularly critical. The circuits have been successfully constructed using both electrolytic and stacked film capacitors and can be made very compact. In principle, they are also suitable for integration if the passive components are scaled appropriately. In this sense, the present circuits offer an egalitarian version of chaos, accessible to an experimenter or an enthusiast, while still providing insight to an engineer or a theoretician.

ACKNOWLEDGMENT

J. Piper would like to thank Dr. C. Thompson and Dr. K. Kiers for their valuable feedback.

REFERENCES

[1] P. S. Linsay, "Period doubling and chaotic behavior in a driven anharmonic oscillator," *Phys. Rev. Lett.*, vol. 47, no. 19, pp. 1349–1352, 1981.
[2] J. H. B. Deane, "Modeling the dynamics of nonlinear inductor circuits," *IEEE Trans. Magn.*, vol. 30, no. 5, pp. 2795–2801, Sep. 1994.
[3] K. Murali, M. Lakshmanan, and L. O. Chua, "The simplest dissipative nonautonomous chaotic circuit," *IEEE Trans. Circuits Syst. I, Fundam. Theory Appl.*, vol. 41, no. 6, pp. 462–463, Jun. 1994.
[4] E. Lindberg, K. Murali, and A. Tamasevicius, "The smallest transistor-based nonautonomous chaotic circuit," *IEEE Trans. Circuits Syst. II, Exp. Briefs*, vol. 52, no. 10, pp. 661–664, Oct. 2005.
[5] T. Matsumoto, "A chaotic attractor from Chua's circuit," *IEEE Trans. Circuits Syst.*, vol. CAS-31, no. 12, pp. 1055–1058, Dec. 1984.
[6] T. Tsubone and T. Saito, "Stabilizing and destabilizing control for a piecewise-linear circuit," *IEEE Trans. Circuits Syst. I, Fundam. Theory Appl.*, vol. 45, no. 2, pp. 172–177, Feb. 1998.
[7] J. C. Sprott, "Simple chaotic systems and circuits," *Amer. J. Phys.*, vol. 68, no. 8, pp. 758–763, 2000.
[8] A. Elwakil and M. P. Kennedy, "Construction of classes of circuit-independent chaotic oscillators using passive-only nonlinear devices," *IEEE Trans. Circuits Syst. I, Fundam. Theory Appl.*, vol. 48, no. 3, pp. 289–307, Mar. 2001.
[9] J. C. Sprott, *Chaos and Time Series Analysis*. New York: Oxford Univ. Press, 2003.
[10] J. C. Sprott, *Elegant Chaos: Algebraically Simple Chaotic Flows*. Singapore: World Scientific, 2010.